Biophysical Journal Volume 104 June 2013 2476–2484

# Fracture Mechanics of Collagen Fibrils: Influence of Natural Cross-Links

Rene B. Svensson,[†‡*] Hindrik Mulder,[§] Vuokko Kovanen,[¶] and S. Peter Magnusson[†]
[†]Institute of Sports Medicine Copenhagen, Bispebjerg Hospital and Center for Healthy Aging, Faculty of Health Sciences and [‡]Nano-Science Center, Faculty of Science, University of Copenhagen, Copenhagen, Denmark; [§]Unit of Molecular Metabolism, Department of Clinical Sciences, Lund University, Malmö, Sweden; and [¶]Gerontology Research Center, Department of Health Sciences, University of Jyväskylä, Jyväskylä, Finland

ABSTRACT Tendons are important load-bearing structures, which are frequently injured in both sports and work. Type I collagen fibrils are the primary components of tendons and carry most of the mechanical loads experienced by the tissue, however, knowledge of how load is transmitted between and within fibrils is limited. The presence of covalent enzymatic cross-links between collagen molecules is an important factor that has been shown to influence mechanical behavior of the tendons. To improve our understanding of how molecular bonds translate into tendon mechanics, we used an atomic force microscopy technique to measure the mechanical behavior of individual collagen fibrils loaded to failure. Fibrils from human patellar tendons, rat-tail tendons (RTTs), $NaBH_4$ reduced RTTs, and tail tendons of Zucker diabetic fat rats were tested. We found a characteristic three-phase stress-strain behavior in the human collagen fibrils. There was an initial rise in modulus followed by a plateau with reduced modulus, which was finally followed by an even greater increase in stress and modulus before failure. The RTTs also displayed the initial increase and plateau phase, but the third region was virtually absent and the plateau continued until failure. The importance of cross-link lability was investigated by $NaBH_4$ reduction of the rat-tail fibrils, which did not alter their behavior. These findings shed light on the function of cross-links at the fibril level, but further studies will be required to establish the underlying mechanisms.

## INTRODUCTION

Mechanical stability and function of humans and other higher organisms are made possible by connective tissues that carry both tensile and compressive loads. Despite differences in structures and loading conditions, connective tissues are to a large extent all based on the same family of proteins, namely collagens (1,2). One of the most collagen-rich connective tissues is tendons, which connect muscles to bones across joints, and thereby enable muscle-generated forces to create movement (3). Because tendons often operate with a short moment arm, some tendons can experience very large loads, up to ~400 kg during jumping (4). Such highly loaded tendons operate with a fairly low safety margin making them a common site of both sports and work-related injuries (5–7).

The central part of a tendon consists mainly of fibrillar type I collagen (8,9). The type I collagen molecule is a 300 nm long triple helix consisting of two $\alpha$1 and one $\alpha$2 chains. The molecules assemble by staggered lateral aggregation into thin (20–500 nm) and long (probably $>$1 mm) fibrils (10–13). In tendon, almost all fibrils are aligned in parallel to transmit unidirectional tension, whereas other tissues have different organizations depending on shape and mechanical loading. The nonhelical ends (telopeptides) of collagen molecules are involved in the formation of intermolecular covalent cross-links within the fibril (14).

There are two basic types of natural cross-links: enzymatic and advanced glycation end-products (AGEs). Enzymatic cross-links are essential in the formation of functional collagen fibrils, whereas AGEs accumulate with age and diabetes and may impair normal function (15,16). Cross-linking directly affects the mechanical function of connective tissues (14,17,18) and also affects tissue biochemistry, making collagen less susceptible to proteolytic degradation (19,20). This makes cross-links an important parameter in connective tissue behavior, especially as it relates to ageing and diabetes.

Enzymatic cross-link formation is initiated by the enzyme lysyl oxidase acting on specific lysines in the telopeptides (14). The resulting allysine reacts rapidly with a specific lysine in the helical region of a neighboring molecule to form an immature divalent intermolecular bond (21,22). Over time, immature cross-links can react with an additional telopeptide allysine to form a trivalent mature bond (14,23). Whether the additional bond is intra- or intermolecular is still unknown, however, the latter is expected to enhance mechanical strength to a greater extent than the former. In addition to this main pathway of cross-link formation, other cross-links may form from the reaction of allysines, lysines, and histidines. Significant variations in cross-link types have been reported in different tissues and for example adult human patellar tendon (HPT) contains significant amounts of mature trivalent hydroxylysyl pyridinoline (HP) cross-links (24). By comparison RTT is dominated by divalent immature dehydro-hydroxylysinonorleucine (deH-HLN) cross-links and possibly trivalent dehydro-hydroxymerodesmosine (deH-HMD) or tetravalent dehydro-histidinohydroxymerodesmosine (deH-HHMD) all of which are acid labile (25–27). Consequently, RTT collagen is highly

*Submitted February 20, 2013, and accepted for publication April 17, 2013.*
*Correspondence: svensson.nano@gmail.com
Editor: Charles Wolgemuth.

0006-3495/13/06/2476/9 $2.00
http://dx.doi.org/10.1016/j.bpj.2013.04.033

soluble in dilute acid. The lack of stable mature cross-links is likely related to the low mechanical load on tail tendons because mechanically loaded rat tendons like the Achilles do contain mature cross-links (28).

AGE cross-links are formed by reactions with reducing sugars, such as glucose (29). This type of reaction is largely unspecific, producing both cross-linking and noncross-linking compounds along the protein. The amount of AGEs formed on a protein increases with time until it is degraded. This allows large amounts of AGEs to accumulate due to the extensive half-life of collagen (30,31). AGEs have also been implicated in the development of the late complications of diabetes, where plasma glucose levels are elevated permitting extensive AGE formation. The complications mainly arise in the microvasculature of the kidneys, retina, and perhaps neural vasculature (32).

Although the collagen fibril is the structural level at which natural cross-links function, measurements of their mechanical influence at this level have not previously been described. In this work, we investigate the ultimate tensile properties of collagen fibrils from human patellar tendons (containing mature enzymatic cross-links) and rat-tail tendons (dominated by immature enzymatic cross-links). We relate our findings to cross-link type and stability. To our knowledge, the failure properties of human collagen fibrils have not been reported before.

## MATERIALS AND METHODS

### Materials

HPT tissue was obtained during anterior cruciate ligament autograft surgery on three otherwise healthy males (33–39 years of age). Surgery took place 4–6 months postinjury and the subjects underwent rehabilitation before the surgery, ensuring that the patellar tendon did not suffer from disuse. All subjects gave their informed consent. Samples were wrapped in phosphate buffered saline (PBS)-soaked gauze and stored frozen at –20°C.

Tails of three healthy 12-week-old female Wistar rats and two 16-week-old Zucker diabetic fat (ZDF) rats were stored frozen at –20°C. After thawing, several fascicles were extracted from the distal end. The fascicles were wrapped in PBS-soaked gauze and stored at –20°C until use. Tissue collection was approved by the local ethics committee.

### $NaBH_4$ reduction

The immature deH-HLN cross-links found in RTT contain an imine bond, which is labile in acid but can be reduced to a stable amine in the HLN cross-link (27). Regardless of whether deH-HMD or deH-HHMD is present in native RTT, reduction at neutral pH will form the stable HHMD cross-link (25). Some of the RTT fascicles were reduced with $NaBH_4$ to stabilize their immature cross-links. Nine mg $NaBH_4$ (Sigma Aldrich, St. Louis, MO) was dissolved in 2 mL of 0.15 mM NaOH. Fascicles were placed in 10 mL of 150 mM phosphate buffer (pH = 7.4) and 0.5 mL of the $NaBH_4$ solution was added every 15 min for 1 h while stirring. After treatment, the fascicles were washed twice by placing them in 5 mL of 150 mM phosphate buffer and stirring for 5 min. Mechanical testing of fascicles was performed immediately after treatment, whereas tissue for all other tests was stored on 150 mM PBS-soaked gauze at –20°C until use.

### Acid solubility

Collagen fascicles were dissolved in 3.5 mL of 0.05 M acetic acid for 20 h at ~5°C. The resulting solution was ultracentrifuged at 100,000 × $g$ for 1 h at 4°C after which 3 mL of the supernatant was removed leaving 0.5 mL of solute with the gel-like pellet (26). Collagen content in the two fractions was determined by a colorimetric hydroxyproline assay using chloramine-T oxidation and reading color reaction with 4-dimethylaminobenzaldehyde at 570 nm (33). Solubility was expressed as the supernatant hydroxyproline fraction of the total content. The calculated hydroxyproline content of 0.5 mL supernatant was subtracted from the pellet value and added to the total supernatant content to account for the solute left with the pellet.

### Cross-link and collagen content

Concentrations of HP, lysyl pyridinoline (LP), and pentosidine (PENT) were analyzed by high-performance liquid chromatography as previously reported (34). Values are normalized to collagen content measured by a spectrophotometric assay assuming 13.7% hydroxyproline by mass in collagen (35).

### Mechanical testing

Mechanical testing of collagen fibrils, using atomic force microscopy (AFM), was performed similarly to our previously published method (36). In brief, a small piece of tissue was gently sheared apart on a silicon substrate under a droplet of PBS to deposit collagen fibrils. The sample was rinsed in deionized water and dried under nitrogen flow. A solitary fibril was located under an optical microscope and droplets of epoxy were applied along the fibril using an AFM cantilever. After curing over night an AFM cantilever was used to scrape one droplet free from the substrate and flip it over, the cantilever used for mechanical testing was then attached with fresh epoxy to the flipped droplet, effectively sandwiching the fibril between the cantilever and flipped droplet. After curing over night the sample was rehydrated in PBS and the fibril was mechanically tested (36). To test fibrils to failure, our previously published method was modified as follows. The system is limited to 20 $\mu$m deformation, which only allowed failure testing of short fibril segments <40 $\mu$m. Use of a stiff AFM cantilever (OMCL-AC160TS, spring constant ~42 N/m, Olympus, Tokyo, Japan) enabled measurement of the entire force range up to failure. The long tip (10 $\mu$m) on this cantilever type hindered glue deposition at the cantilever end and therefore the tip was removed by mechanically breaking it against a sharp silicon edge.

Despite the stiff cantilever, deflection often exceeded the linear range of the detector ($\pm$3 V), and therefore the detector nonlinearity was determined by engaging on a hard silicon substrate to produce a linear deflection versus distance response. Deviation of the detector signal from linearity was well described by a 3rd order polynomial. The fit to three such measurements made on three separate days and cantilevers was used to correct all measured deflection values (see Fig. 1 *B*). The cantilever deflection sensitivity was determined in the dry state before glue was deposited on the cantilever. To determine the corresponding wet deflection sensitivity, an experiment was performed to measure sensitivity both dry and wet at various laser positions along the cantilever. A linear relation between dry and wet sensitivity was found and used to calculate wet values (Fig. 1 *A*).

Collagen fibrils were tested at various strain rates in the low strain range (~5%) (results not reported here), which functioned as preconditioning. The failure test consisted of a single pull to failure at a speed of 40 $\mu$m/s (~100%/s strain rate).

Due to equipment breakdown, ZDF rats were tested on a different AFM (MFP-3D, Asylum Research, Santa Barbara, CA). The described method was used except that wet deflection sensitivity was measured directly in mQ water before each experiment.

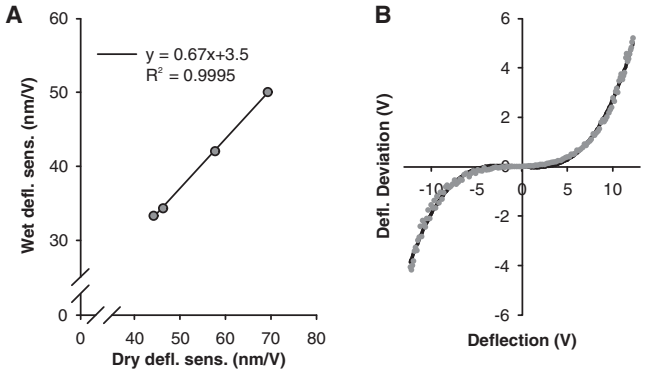


FIGURE 1 (*A*) Relation between AFM deflection sensitivity in wet and dry conditions, including a linear fit. (*B*) Deviation from linearity of the detector as a function of the measured deflection voltage. Dots are data from three separate measurements (down sampled 40× for clarity) and the line is a 3rd order polynomial fit.

For comparison, mechanical testing at the fascicle level on native-RTT (N-RTT) and reduced-RTT (R-RTT) was performed in a Deben microtensile rig as previously reported (36). Three preconditioning cycles to 2% strain were performed before stretching to failure. The gauge length was 2 cm and the deformation rate was 2 mm/min.

## Fibril imaging

Tapping mode AFM imaging in air was performed before mechanical testing to determine the dry cross-sectional area (CSA) and ensure structural integrity of collagen fibrils. When possible the remaining piece of fibril on the sample after the mechanical test was also imaged to investigate the structure.

## Data analysis and statistics

Mechanical data were analyzed using one-way analysis of variance and posttests employed Tukey's correction for multiple comparisons. Breakage site and fibril disruption were analyzed by table analysis using a Fisher's exact binomial test for significance. A significance level of 0.05 was used. Measured values were reported as mean ± standard deviation and group differences were reported as mean difference with 95% confidence intervals. For HPT $N = 7$ fibrils from three different persons. For N-RTT $N = 8$ fibrils from three different rats. For reduced R-RTT $N = 6$ fibrils from the same three rats as N-RTT. For ZDF-RTT $N = 4$ fibrils from two different rats.

## End-effects

Material properties can usually be assumed independent of specimen dimensions. By pooling the present data obtained on short HPT fibrils with data from our previous works on longer fibrils (36,37), we observed a clear increase in low strain (~4%) modulus with increasing length (Fig. 2 *A*). The most likely explanation for this is the presence of so-called end-effects related to deformation in the gripping regions at the ends of the specimen. With the present method part of the end-effects are likely related to fibril bending due to the geometry of the grip. As a simple model the end-effects can be incorporated as an added spring element in series with the specimen. The specimen may change length and CSA, whereas the end-spring does not change length but possibly follows the CSA of the specimen. The compliance of two serially connected springs is

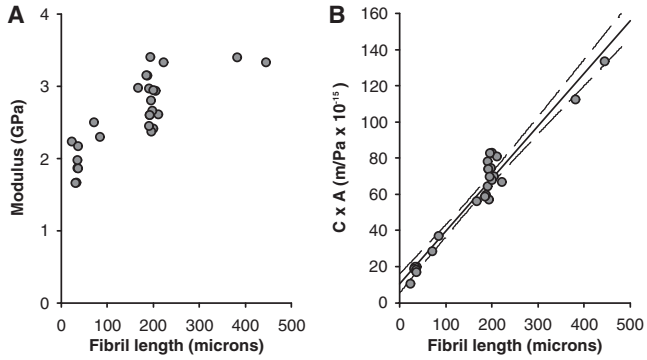


FIGURE 2 (*A*) Across our present and previous measurements, we observe an increase in collagen fibril modulus with the length of the tested specimen. (*B*) Plot of the fibril compliance multiplied with fibril CSA ($C \times A$) as a function of fibril length, including a linear fit (see text for details).

$$C = \frac{1}{k} = \frac{1}{k_{end}} + \frac{1}{k_{fib}} = \frac{l_{end}}{A_{end} \times E_{end}} + \frac{l_{fib}}{A_{fib} \times E_{fib}}$$

$$\Rightarrow C \times A_{fib} = \frac{l_{end}}{A_{end} \times E_{end}} \times A_{fib} + \frac{1}{E_{fib}} \times l_{fib}.$$

Here, $C$ is the compliance, $k$ is the spring constant, $l$ is the length, $A$ is the CSA, and $E$ is the elastic modulus. Subscripts *end* and *fib* designate the end-effect element and the fibril, respectively. From this a 3D plot of $C \times A_{fib}$ versus fibril length and CSA should give a plane, however, we found that the CSA dependence was small suggesting that $A_{end}$ is proportional to $A_{fib}$, which simplifies the relation to give

$$C \times A_{fib} = \frac{l_{end} \times K_{prop}}{E_{end}} + \frac{1}{E_{fib}} \times l_{fib},$$

where $K_{prop}$ is the constant of proportionality. Plotting $C \times A_{fib}$ versus fibril length thus yields a straight line with the slope given by the inverse of fibril modulus and the intersect defining the magnitude of the end-effects (Fig. 2 *B*). From this a fibril modulus of 3.4 GPa is predicted and given the mean modulus of short HPT fibrils, in this study (1.9 GPa) we estimate that ~45% of the measured strains are due to end-effects.

To present data as close to the true value as possible we have included this correction to the strains. It should be noted that this is a simple multiplicative factor and the original measured values can be obtained by dividing reported strains and multiplying reported modulus values by 0.55.

# RESULTS

## Acid solubility, collagen content, and cross-links

The results of the biochemical analyses are shown in Table 1. Solubility in dilute acetic acid was significantly lower in

**TABLE 1 Biochemical parameters (mean ± SD)**

| | HPT | N-RTT | ZDF-RTT | R-RTT |
|---|---|---|---|---|
| Acid solubility (%) | 4.5 ± 0.3 | 89 ± 7 | 90 ± 7 | <1 |
| Collagen content (%) | 67 ± 8 | 87 ± 7 | 85 ± 3 | – |
| HP (mmol/mol)[a] | 890 ± 250 | 8.7 ± 2.9 | 9.4 ± 0.5 | – |
| LP (mmol/mol)[a] | 23 ± 5 | 4.5 ± 0.4 | 4.4 ± 0.4 | – |
| PENT (mmol/mol)[a] | 26 ± 3 | 0.071 ± 0.024 | 0.083 ± 0.005 | – |

[a]Cross-link values in RTT were near the detection limit and absolute values should be regarded with some caution.

HPT compared to N-RTT and ZDF-RTT, but there was no difference between N-RTT and ZDF-RTT. Reduction by $NaBH_4$ made the R-RTT collagen practically insoluble (dissolved hydroxyproline was below the detection limit). Mature cross-links HP and LP were significantly more abundant in HPT than any of the RTT tissues. The same was the case for the marker of advanced glycation PENT. The N-RTT and ZDF-RTT did not differ in any of the cross-links. Collagen content was significantly lower in HPT than the RTT tissues.

### HPT fibril mechanics

Fibrils from HPT displayed three distinct phases in the mechanical response up to failure (Fig. 3). In region I (~0–7% strain) the modulus increased with strain reaching a peak value (Mod1) around which the stress-strain response was fairly linear. In region II (~7–15% strain), the modulus dropped resulting in a flattening of the stress-strain curve. Finally, in region III (~15–25% strain), the modulus started increasing again and continued to do so until ultimate failure, at which point the peak modulus (Mod2) usually exceeded that in region I. The mechanical parameters are summarized in Table 2.

### RTT fibril mechanics

The mechanical behavior of collagen fibrils from RTT was different from that observed in HPT fibrils (Fig. 4). Like the HPT fibrils, modulus increased with strain in region I leading up to a peak value after which the modulus decreased in region II. However, unlike HPT fibrils, the modulus increase in region III was either absent or less distinct, reaching a lower value than in region I. Mechanical parameters are summarized in Table 2. Both the R-RTT and ZDF-RTT behaved similarly to the N-RTT fibrils, and thus differently from HPT fibrils (Fig. 4, *C* and *D*).

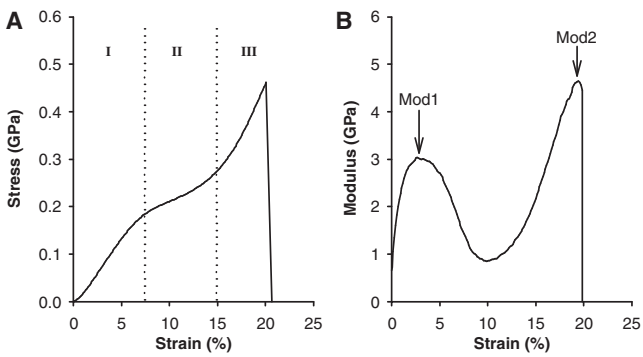


FIGURE 3 (*A*) Stress-strain response of a representative HPT collagen fibril. Three distinct regions (denoted I, II, and III) are observed. (*B*) The local modulus of the same curve as a function of strain. The three regions give rise to two distinct peak modulus values, Mod1 and Mod2.

### Mechanical effects

Mechanical differences between the groups in region I (linear) and region III (failure) are reported in Table 3. Differences in region II (middle plateau) are not included because the region was poorly defined in RTT, which displayed plateau all the way to failure. Neither the reduced nor the ZDF RTT differed significantly from native RTT in any of the mechanical parameters. It should be noted that the confidence intervals are wide and differences of a functionally relevant magnitude may be hidden (e.g., a type II error). HPT fibrils had a significantly higher modulus in region I (Mod1) than the native RTT fibrils. In region III, both modulus (Mod2) and failure stress were significantly higher (Table 3). Mod2 was greater than Mod1 for HPT fibrils in contrast to native RTT fibrils, which had a lower Mod2 than Mod1.

Because all the RTT groups behaved similarly, they were also pooled (RTT-all). Significant differences to the HPT fibrils were seen in the same parameters as for the native RTT, with the addition of failure strain also being significantly higher in HPT fibrils (Table 3).

### Structural effects

Two different structures were observed on the broken fibrils. Some were relatively intact and retained D-banding along the entire fibril up to the breakage site, whereas others displayed gross disruption of fibril structure throughout the length (Fig. 5). Twenty fibrils could be imaged of which 10 had intact structure and 10 were disrupted. Breakage site (mid or end) was assessed from the length of the broken fibril compared to the original length in 23 fibrils. Failure in the midsubstance occurred in 14 fibrils and 9 had failed at the end.

Using Fisher's exact test, a significant ($p = 0.008$) relationship between breakage site and structure of the broken fibril was found. Of the end-failures, 100% were intact and 69% of the midsubstance failures were disrupted (Table 4). Tissue origin also tended to relate to failure site and structure such that HPT fibrils had predominantly intact end failures and rat fibrils had disrupted midsubstance failures, however, these relationships were not significant. None of the mechanical parameters were significantly related to breakage site or structure when the confounding factor of tissue origin was accounted for.

### Fascicle mechanics

The N-RTT fascicles displayed a behavior somewhat similar to that of the fibrils with an initial high modulus (1.4 ± 0.3 GPa) followed by a plateau region up to failure that occurred at 11 ± 3% strain and 38 ± 10 MPa stress (Fig. 6). R-RTT fascicles had a markedly different mechanical response with no plateau region but a similar initial modulus

**TABLE 2 Structural and mechanical parameters (mean ± SD)**

| | HPT | N-RTT | R-RTT | ZDF-RTT | RTT-all |
|---|---|---|---|---|---|
| Tested length ($\mu$m) | 33 ± 5 | 34 ± 4 | 37 ± 5 | 32 ± 2 | 35 ± 4 |
| CSA ($\mu m^2$) | 0.021 ± 0.004 | 0.033 ± 0.018 | 0.031 ± 0.011 | 0.025 ± 0.006 | 0.036 ± 0.014 |
| Mod1 (GPa) | 3.5 ± 0.4 | 2.2 ± 0.9 | 2.9 ± 0.4 | 2.9 ± 0.5 | 2.6 ± 0.7 |
| Mod1 strain (%) | 3.3 ± 1.1 | 4.6 ± 2.8 | 4.0 ± 0.9 | 5.7 ± 2.5 | 4.6 ± 2.2 |
| Mod2 (GPa)[a] | 4.3 ± 1.4 | 1.4 ± 0.7 | 1.5 ± 0.5 | 1.9 ± 0.5 | 1.6 ± 0.6 |
| Ultimate stress (MPa) | 540 ± 140 | 200 ± 110 | 290 ± 80 | 270 ± 60 | 250 ± 100 |
| Ultimate strain (%) | 20 ± 1 | 16 ± 4 | 19 ± 4 | 16.5 ± 2 | 17 ± 4 |
| Mod2/Mod1[a] | 1.24 ± 0.35 | 0.60 ± 0.30 | 0.51 ± 0.18 | 0.73 ± 0.34 | 0.59 ± 0.26 |

[a]Not all RTT fibrils showed the 2nd modulus increase, presented data are for 5 N-RTT, 5 R-RTT, and 3 ZDF-RTT fibrils that show the increase.

(1.5 ± 0.3 GPa) and a more brittle failure with lower strain (5.0 ± 0.8%, $p = 0.009$) and higher stress (58 ± 18 MPa, $p = 0.04$). We also observed that after failure, the N-RTT fascicles appeared to have lost their crimp structure, whereas the R-RTT fascicles still retained their crimps. In addition, all the N-RTT fascicles failed in the midsubstance, whereas the R-RTT fascicles failed close to the clamp.

## DISCUSSION

Cross-linking in collagen is believed to be a major source of mechanical strength in connective tissues, and improved mechanical properties during development is likely related to maturation of enzymatic cross-links (14). Native RTT collagen contains mostly immature cross-links, as evidenced by the high acid solubility, whereas adult HPT collagen contains significant amounts of mature cross-links (24,27). Our results showed that these two tissues also differ markedly in their mechanical response at the fibril level. The differences in mechanical behavior occurred predominantly at the high strain level in region III. RTT fibrils displayed a longer plateau, whereas HPT fibrils had a significant rise in stress and modulus (Fig. 4). A relation between poor cross-linking and the occurrence of a plateau in the stress-strain response has been reported at the fascicle level in rats treated with $\beta$-aminopropionitrile, which suppresses lysyl oxidase activity and thereby enzymatic cross-link formation (17). A plateau in the mechanical response leading up to failure was also recently reported by molecular modeling (38). In addition to the mechanical differences there was also a tendency for more extensive disruption of the fibril structure in RTT, which may indicate a change in failure mechanism. Care must be taken when comparing results across different species because numerous factors may be dissimilar, however, we believe that the large difference in cross-linking is a plausible explanation for the mechanical differences in region III and greater structural disruption, although it remains to be confirmed.

The present observations cannot establish the mechanism responsible for the observed behavior, but these may include helix uncoiling and molecular slippage. A three-phase behavior similar to the present one has previously been reported in the uncoiling of myosin II tails (39). Here, the coiled-coil initially resists force until a threshold is reached where the coil begins to unfold giving rise to a plateau. The plateau extends until backbone stretching becomes dominant, which leads to a second increase in modulus. An alternative mechanism may involve molecular slippage rather than unfolding in the plateau phase. In this case such slippage would be halted by intermolecular cross-links and give rise to the increased modulus in region III. A recently reported modeling study found a three-phase behavior for two collagen molecules connected by a single cross-link where slippage was accommodated by straightening of a hairpin loop found at the $\alpha$1(I) C-telopeptide (40). Regardless of the mechanism, the plateau may have a physiological function to increase the toughness of the fibril and reducing the risk of brittle failure.

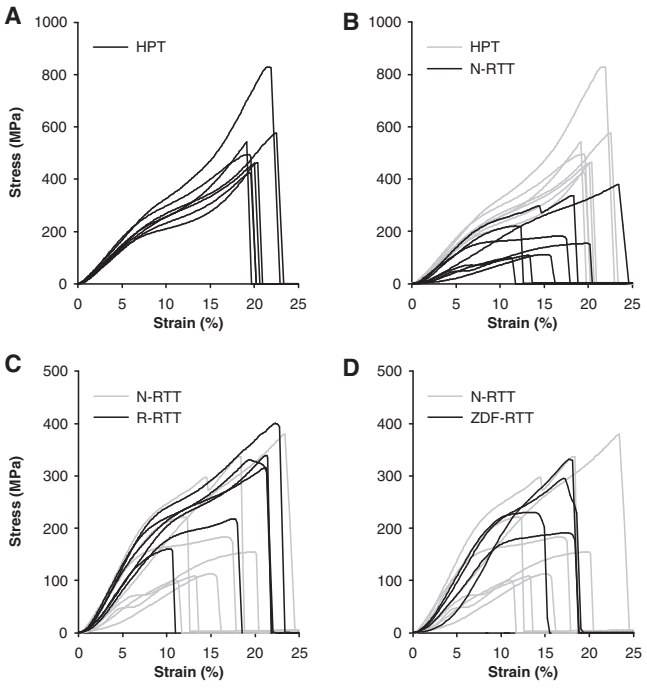


FIGURE 4 Mechanical response of (*A*) HPT collagen fibrils. (*B*) Native RTT fibrils (*black*) compared to the HPT fibrils (*gray*). (*C*) Reduced RTT (*black*) compared to native RTT (*gray*). (*D*) ZDF RTT (*black*) compared to native RTT (*gray*).

**TABLE 3 Mechanical differences between groups (mean difference (95% confidence interval))**

| | Effect of reduction: R-RTT – N-RTT | Effect of diabetes: ZDF-RTT – N-RTT | Effect of Tissue: HPT – N-RTT | Pooled RTT: HPT – RTT-all |
|---|---|---|---|---|
| Mod1 (GPa) | +0.67 (−0.27–1.61) | +0.71 (−0.35–1.78) | +1.29 (0.38–2.19)[a] | +0.90 (0.29–1.52)[a] |
| Mod1 strain (%) | −0.5 (−3.5–2.5) | +1.1 (−2.4–4.5) | −1.3 (−3.8–2.4) | −1.3 (−3.2–0.5) |
| Mod2 (GPa) | +0.11 (−1.64–1.85) | +0.55 (−1.47–2.57) | +2.93 (1.31–4.54)[a] | +2.76 (1.84–3.67)[a] |
| Ultimate stress (MPa) | +90 (−70–260) | +70 (−110–250) | +340 (190–500)[a] | +300 (200–400)[a] |
| Ultimate strain (%) | +2.6 (−2.6–7.7) | +0.4 (−5.4–6.3) | +4.3 (−0.6–9.3) | +3.4 (0.2–6.5)[a] |
| Mod2/Mod1 | −0.09 (−0.64–0.46) | +0.13 (−0.50–0.76) | +0.64 (0.13–1.15)[a] | +0.64 (0.35–0.93)[a] |

[a]Statistically significant ($p < 0.05$).

Immature cross-links differ from mature by having a labile imine bond. We speculated that the reduced strength in RTT fibrils compared to HPT was caused by breakage of the labile bonds. To test this hypothesis, we treated RTT fascicles with $NaBH_4$ to stabilize the bond (41–43). The treatment was efficient in stabilizing the immature cross-links as seen from the lack of acid solubility. However, although there was a tendency toward increased modulus in region I and higher failure stress, there was no effect on the curve shape in region III (Fig. 4 *C*). Because the difference between RTT and HPT could not be explained by lability alone, other factors must also be involved. These could be related to other aspects of the mature cross-links in HPT than their stability but other differences in composition and microstructure between the tissues may also be involved.

The modest effect of $NaBH_4$ treatment at the fibril level is in contrast to the fascicle results, which show a marked change in mechanical behavior toward greater brittleness. Previous reports have found similar changes with reduction at the fascicle level (41), and it was proposed that these effects were caused by changes at the fibril level due to stabilized cross-links. Our findings at the fibril level suggest that inter- rather than intrafibrillar connectivity give rise to the effects at the fascicle level. However, we did not observe any noticeable difficulty in separating fibrils for AFM after the treatment, which indicates that interfibrillar bonding was not enhanced. An alternative possibility could be that the fibrils we sampled were not representative of the tissue. For technical reasons, we were only able to test fibrils of ~100 nm diameter or larger, however, in RTT most of the fibrils are of this size. Another issue of selection could be that we only use fibrils that are structurally intact, which may discard the weaker fibrils, but only a small portion of the fibrils displayed structural disruption so the bias on account of this should be minor.

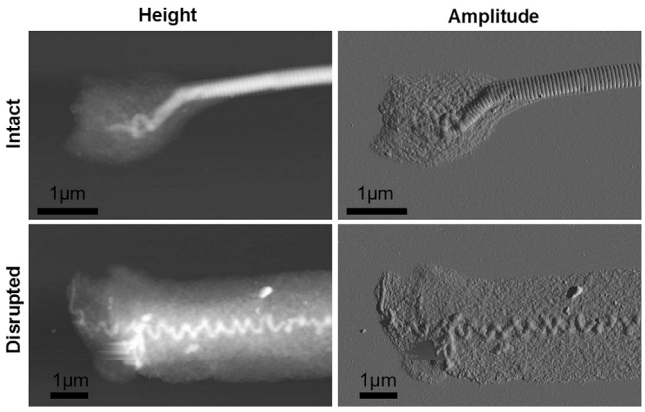


FIGURE 5 Height and amplitude AFM images of collagen fibril breakage sites after failure testing. A failure mode with a largely intact fibril and one with a heavily disrupted fibril was observed (the structure present toward the right of the images continues throughout the rest of the fibril).

In addition to the difference in cross-link maturity, the HPT also had much higher levels of AGE cross-linking than RTT as evaluated by PENT concentration (Table 1). We intended to elucidate this by including the hyperglycemic ZDF rats, however, it turned out that they did not exhibit more AGE cross-links than the normal RTT. It is therefore not surprising that the ZDF fibrils behaved similar to the normal ones. Based on this behavior, we cannot rule out that AGE cross-links could be responsible for the observed difference between the HPT and RTT fibrils. However, because age-related changes to tendon mechanics are relatively moderate and glycation-related pathology is not expected at the age of our HPT donors (36 ± 3 years), we still expect the primary cause of the difference to be enzymatic cross-link maturity. We intend to investigate the effects of AGE formation in greater detail in a future study.

To our knowledge, only one previous study by Yang et al. (44) has investigated failure properties of mammalian collagen fibrils. In that study, native collagen fibrils from bovine Achilles tendons were reported to fail at a strain of 13% and a stress of 60 MPa (~135 MPa using dry CSA, based on ~50% swelling as reported (44)). We suspect

**TABLE 4 Fibril breakage site and structure after failure (number of fibrils)**

| | Disrupted | Intact |
|---|---|---|
| End | 0 | 6 |
| Mid | 9 | 4 |
| | **Disrupted** | **Intact** |
| HPT | 1 | 4 |
| RTT | 9 | 6 |
| | **End** | **Mid** |
| HPT | 4 | 2 |
| RTT | 5 | 12 |

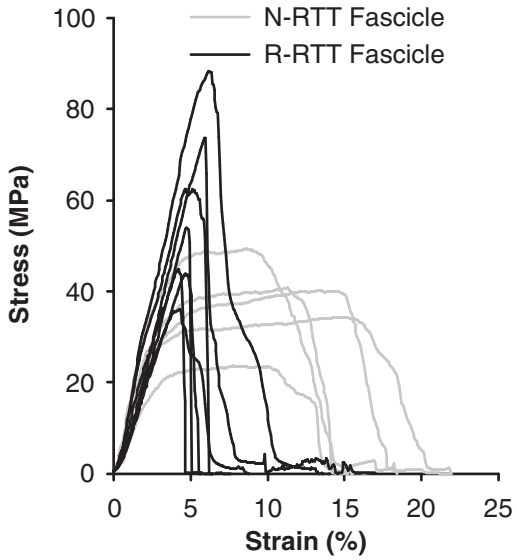


FIGURE 6 Mechanical response of untreated (*gray*) and $NaBH_4$ treated (*black*) fascicles.

that the lower values of failure stress and strain compared to the present findings may be due to the preparation by Yang et al. (45), which involves swelling in 0.01 M HCl overnight. In the same work, cross-linking agents were found to improve mechanical properties, with glutaraldehyde treatment increasing failure strain to 22% and stress to 290 MPa (~650 MPa using dry CSA). These values are well in line with our findings; however, Yang et al. did not find the three distinct regions that we observed in HPT fibrils.

Collagen fibril failure properties have also been reported on fibrils from sea cucumber, however, these behave significantly different from fibrils in this work, failing at a much higher strain of 80% and a stress of 230 MPa (~1.1 GPa using dry CSA) and also displaying quite different stress-strain behavior (46). However, it is difficult to compare these fibrils with the mammalian ones in this work because echinoderm fibrils have significantly different structure (47).

### Relation to tendon failure

To compare the present failure properties of fibrils to those of tendons it is necessary to account for the fibril content in the tendon. Using a fibril swelling of 30% at physiological hydration and a fibril volume fraction in tendon of 60%, the stress and modulus of fibrils must be divided by 2.8 to compare with tendon values (see (37) for details). For the RTT fibrils this normalization yields a failure stress of 90 MPa with a corresponding strain of 17%. In comparison, the fascicles from which the fibrils were obtained failed at 35 MPa stress and 10% strain, which is in the low end of previously reported values (~50–110 MPa stress and 12–20% strain (48–50)), likely due to the young rats in this study. For the HPT fibrils the failure stress and strain normalized to the tendon level becomes 190 MPa and 20%, respectively. The strain is within the ~10–25% that has been reported for HPTs and fascicles but the fibril stress is markedly greater than the ~30–90 MPa found at the macroscopic level (51–54). The lower strength in both RTT and HPT fascicles compared to fibrils could indicate that tendons fail by fibril slippage rather than breakage, but other explanations should also be considered. First, the risk of having a local defect within the short fibril segments that we tested is much lower than in a full-length native fibril. The native fibril may therefore be weaker than predicted by our measurements (55). Second, fibrils are not evenly loaded within the tendon but are sequentially recruited throughout the toe region and the stress on some fibrils may therefore exceed their failure strength although the overall mean stress does not (56). Such sequential breakage of fibrils would lead to a lower ultimate stress.

## CONCLUSIONS

There was a clear difference in mechanical behavior between collagen fibrils from mature HPTs and from RTTs. The human fibrils displayed a region of increasing modulus at high strains before abrupt failure. In contrast RTTs displayed a plateau leading up to failure. Because of these different curve shapes, human fibrils failed at significantly higher stress than rat-tail fibrils. We propose that these mechanical observations relate to the prominent differences in cross-link maturity of the tissues. By $NaBH_4$ reduction we determined that immature cross-link lability was not the primary cause of the mechanical difference. Further investigation is required to determine what other factors may be the cause. Rat-tails are a common tendon model in research but it is important to appreciate the differences in both cross-linking and fibril mechanics as reported here when comparing to load-bearing tendons.

We thank Michael Krogsgaard, MD, PhD, Orthopedic Dept., Bispebjerg Hospital, Copenhagen, Denmark, for collecting biopsy tissue during routine anterior cruciate ligament construction, and Tue Hassenkam, PhD, NanoGeo-Science, Nano-Science Center, University of Copenhagen, Denmark, for access to the MFP-3D microscope. Mrs. Kaisa-Leena Tulla, Department of Health Sciences, University of Jyväskylä, Finland is acknowledged for professional HPLC analyses of collagen cross-links.

This work was supported by the Nordea Foundation (Center for Healthy Ageing), the Novo Nordisk Foundation, the Lundbeck Foundation, and the Danish Medical Research Council (FSS). The funding bodies had no influence on the study.

All authors declare no conflicting interests of any kind.

## REFERENCES

1. van der Rest, M., and R. Garrone. 1991. Collagen family of proteins. *FASEB J.* 5:2814–2823.
2. Exposito, J. Y., U. Valcourt, …, C. Lethias. 2010. The fibrillar collagen family. *Int. J. Mol. Sci.* 11:407–426.

3. Kannus, P. 2000. Structure of the tendon connective tissue. *Scand. J. Med. Sci. Sports.* 10:312–320.
4. Finni, T., P. V. Komi, and V. Lepola. 2000. In vivo human triceps surae and quadriceps femoris muscle function in a squat jump and counter movement jump. *Eur. J. Appl. Physiol.* 83:416–426.
5. Nainzadeh, N., A. Malantic-Lin, …, A. C. Loeser. 1999. Repetitive strain injury (cumulative trauma disorder): causes and treatment. *Mt. Sinai J. Med.* 66:192–196.
6. Lian, O. B., L. Engebretsen, and R. Bahr. 2005. Prevalence of jumper's knee among elite athletes from different sports: a cross-sectional study. *Am. J. Sports Med.* 33:561–567.
7. Ker, R. F., R. M. Alexander, and M. B. Bennett. 1988. Why are mammalian tendons so thick. *J. Zool. (Lond.).* 216:309–324.
8. Epstein, Jr., E. H. 1974. $[\alpha 1(III)]_3$ human skin collagen. Release by pepsin digestion and preponderance in fetal life. *J. Biol. Chem.* 249:3225–3231.
9. Gelse, K., E. Pöschl, and T. Aigner. 2003. Collagens–structure, function, and biosynthesis. *Adv. Drug Deliv. Rev.* 55:1531–1546.
10. Parry, D. A. D., and A. S. Craig. 1977. Quantitative electron microscope observations of the collagen fibrils in rat-tail tendon. *Biopolymers.* 16:1015–1031.
11. Hodge, A. J., and J. A. Petruska. 1963. Recent studies with the electron microscope on ordered aggregates of the tropocollagen macromolecule. *In* Aspects of Protein Structure. G. N. Ramachandran, editor. Academic Press, New York. pp. 299–300.
12. Kadler, K. E., D. F. Holmes, …, J. A. Chapman. 1996. Collagen fibril formation. *Biochem. J.* 316:1–11.
13. Provenzano, P. P., and R. Vanderby, Jr. 2006. Collagen fibril morphology and organization: implications for force transmission in ligament and tendon. *Matrix Biol.* 25:71–84.
14. Bailey, A. J., R. G. Paul, and L. Knott. 1998. Mechanisms of maturation and ageing of collagen. *Mech. Ageing Dev.* 106:1–56.
15. Corman, B., M. Duriez, …, B. I. Levy. 1998. Aminoguanidine prevents age-related arterial stiffening and cardiac hypertrophy. *Proc. Natl. Acad. Sci. USA.* 95:1301–1306.
16. Hammes, H. P., S. Martin, …, M. Brownlee. 1991. Aminoguanidine treatment inhibits the development of experimental diabetic retinopathy. *Proc. Natl. Acad. Sci. USA.* 88:11555–11558.
17. Puxkandl, R., I. Zizak, …, P. Fratzl. 2002. Viscoelastic properties of collagen: synchrotron radiation investigations and structural model. *Philos. Trans. R. Soc. Lond. B Biol. Sci.* 357:191–197.
18. Wagner, D. R., K. M. Reiser, and J. C. Lotz. 2006. Glycation increases human annulus fibrosus stiffness in both experimental measurements and theoretical predictions. *J. Biomech.* 39:1021–1029.
19. Vater, C. A., E. D. Harris, Jr., and R. C. Siegel. 1979. Native cross-links in collagen fibrils induce resistance to human synovial collagenase. *Biochem. J.* 181:639–645.
20. Mott, J. D., R. G. Khalifah, …, B. G. Hudson. 1997. Nonenzymatic glycation of type IV collagen and matrix metalloproteinase susceptibility. *Kidney Int.* 52:1302–1312.
21. Cannon, D. J., and P. F. Davison. 1973. Cross-linking and aging in rat tendon collagen. *Exp. Gerontol.* 8:51–62.
22. Tanzer, M. L. 1968. Intermolecular cross-links in reconstituted collagen fibrils. Evidence for the nature of the covalent bonds. *J. Biol. Chem.* 243:4045–4054.
23. Eyre, D. R., and J. J. Wu. 2005. Collagen cross-links. *Top. Curr. Chem.* 247:207–229.
24. Hansen, P., B. T. Haraldsson, …, S. Peter Magnusson. 2010. Lower strength of the human posterior patellar tendon seems unrelated to mature collagen cross-linking and fibril morphology. *J. Appl. Physiol.* 108:47–52.
25. Robins, S. P., and A. J. Bailey. 1977. The chemistry of the collagen cross-links. Characterization of the products of reduction of skin, tendon and bone with sodium cyanoborohydride. *Biochem. J.* 163:339–346.
26. Yang, S., J. E. Litchfield, and J. W. Baynes. 2003. AGE-breakers cleave model compounds, but do not break Maillard cross-links in skin and tail collagen from diabetic rats. *Arch. Biochem. Biophys.* 412:42–46.
27. Eyre, D. R., M. A. Paz, and P. M. Gallop. 1984. Cross-linking in collagen and elastin. *Annu. Rev. Biochem.* 53:717–748.
28. Carroll, C. C., J. A. Whitt, …, T. L. Broderick. 2012. Influence of acetaminophen consumption and exercise on Achilles tendon structural properties in male Wistar rats. *Am. J. Physiol. Regul. Integr. Comp. Physiol.* 302:R990–R995.
29. Monnier, V. M., and D. R. Sell. 2006. Prevention and repair of protein damage by the Maillard reaction in vivo. *Rejuvenation Res.* 9:264–273.
30. Thorpe, C. T., I. Streeter, …, H. L. Birch. 2010. Aspartic acid racemization and collagen degradation markers reveal an accumulation of damage in tendon collagen that is enhanced with aging. *J. Biol. Chem.* 285:15674–15681.
31. Verzijl, N., J. DeGroot, …, J. M. TeKoppele. 2000. Effect of collagen turnover on the accumulation of advanced glycation end products. *J. Biol. Chem.* 275:39027–39031.
32. Brownlee, M. 2000. Negative consequences of glycation. *Metabolism.* 49(2, Suppl 1):9–13.
33. Syk, I., M. S. Agren, …, B. Jeppsson. 2001. Inhibition of matrix metalloproteinases enhances breaking strength of colonic anastomoses in an experimental model. *Br. J. Surg.* 88:228–234.
34. Kongsgaard, M., V. Kovanen, …, S. P. Magnusson. 2009. Corticosteroid injections, eccentric decline squat training and heavy slow resistance training in patellar tendinopathy. *Scand. J. Med. Sci. Sports.* 19:790–802.
35. Creemers, L. B., D. C. Jansen, …, V. Everts. 1997. Microassay for the assessment of low levels of hydroxyproline. *Biotechniques.* 22:656–658.
36. Svensson, R. B., T. Hassenkam, …, S. P. Magnusson. 2010. Tensile properties of human collagen fibrils and fascicles are insensitive to environmental salts. *Biophys. J.* 99:4020–4027.
37. Svensson, R. B., P. Hansen, …, S. P. Magnusson. 2012. Mechanical properties of human patellar tendon at the hierarchical levels of tendon and fibril. *J. Appl. Physiol.* 112:419–426.
38. Buehler, M. J. 2008. Nanomechanics of collagen fibrils under varying cross-link densities: atomistic and continuum studies. *J. Mech. Behav. Biomed. Mater.* 1:59–67.
39. Schwaiger, I., C. Sattler, …, M. Rief. 2002. The myosin coiled-coil is a truly elastic protein structure. *Nat. Mater.* 1:232–235.
40. Uzel, S. G. M., and M. J. Buehler. 2011. Molecular structure, mechanical behavior and failure mechanism of the C-terminal cross-link domain in type I collagen. *J. Mech. Behav. Biomed. Mater.* 4:153–161.
41. Davison, P. F. 1989. The contribution of labile cross-links to the tensile behavior of tendons. *Connect. Tissue Res.* 18:293–305.
42. Eyre, D. R., M. A. Weis, and J. J. Wu. 2008. Advances in collagen cross-link analysis. *Methods.* 45:65–74.
43. Bailey, A. J. 1968. Intermediate labile intermolecular cross-links in collagen fibres. *Biochim. Biophys. Acta.* 160:447–453.
44. Yang, L., K. O. van der Werf, …, M. L. Bennink. 2012. Micromechanical analysis of native and cross-linked collagen type I fibrils supports the existence of microfibrils. *J. Mech. Behav. Biomed. Mater.* 6:148–158.
45. Yang, L., K. O. van der Werf, …, J. Feijen. 2008. Mechanical properties of native and cross-linked type I collagen fibrils. *Biophys. J.* 94:2204–2211.
46. Shen, Z. L., M. R. Dodge, …, S. J. Eppell. 2010. In vitro fracture testing of submicron diameter collagen fibril specimens. *Biophys. J.* 99:1986–1995.
47. Trotter, J. A., F. A. Thurmond, and T. J. Koob. 1994. Molecular structure and functional morphology of echinoderm collagen fibrils. *Cell Tissue Res.* 275:451–458.
48. Haut, R. C. 1983. Age-dependent influence of strain rate on the tensile failure of rat-tail tendon. *J. Biomech. Eng.* 105:296–299.

49. Silver, F. H., D. L. Christiansen, …, Y. Chen. 2000. Role of storage on changes in the mechanical properties of tendon and self-assembled collagen fibers. *Connect. Tissue Res.* 41:155–164.

50. Gentleman, E., A. N. Lay, …, K. C. Dee. 2003. Mechanical characterization of collagen fibers and scaffolds for tissue engineering. *Biomaterials.* 24:3805–3813.

51. Chun, K. J., and D. L. Butler. 2006. Spatial variation in material properties in fascicle-bone units from human patellar tendon. *In* Experimental Mechanics in Nano and Biotechnology. S. Lee and Y. Kim, editors. Trans Tech Publications, Stafa-Zurich. pp. 797–802.

52. Haraldsson, B. T., P. Aagaard, …, S. P. Magnusson. 2005. Region-specific mechanical properties of the human patella tendon. *J. Appl. Physiol.* 98:1006–1012.

53. Johnson, G. A., D. M. Tramaglini, …, S. L. Woo. 1994. Tensile and viscoelastic properties of human patellar tendon. *J. Orthop. Res.* 12:796–803.

54. Svensson, R. B., T. Hassenkam, …, S. P. Magnusson. 2011. Tensile force transmission in human patellar tendon fascicles is not mediated by glycosaminoglycans. *Connect. Tissue Res.* 52:415–421.

55. Bazant, Z. P. 2004. Scaling theory for quasibrittle structural failure. *Proc. Natl. Acad. Sci. USA.* 101:13400–13407.

56. Bennett, M. B., R. F. Ker, …, R. M. Alexander. 1986. Mechanical properties of various mammalian tendons. *J. Zool.* 209:537–548.